INTERNATIONAL ATOMIC ENERGY AGENCY
UNITED NATIONS EDUCATIONAL, SCIENTIFIC AND CULTURAL ORGANIZATION

INTERNATIONAL CENTRE FOR THEORETICAL PHYSICS
34100 TRIESTE (ITALY) - P.O.B. 586 - MIRAMARE - STRADA COSTIERA 11 - TELEPHONES: 224281/2/3/4/5/6
CABLE: CENTRATOM - TELEX 460392-1

SMR/111 - 1

SECOND SUMMER COLLEGE IN BIOPHYSICS

30 July - 7 September 1984

HIGH RESOLUTION NMR EXPERIMENTS FOR STUDIES OF PROTEIN CONFORMATIONS.

K. Wüthrich
Institut für Molekularbiologie und Biophysik
Eidgenössische Technische Hochschule
ETH-Hönggerberg
CH-8093 Zürich
Switzerland

HIGH RESOLUTION NMR EXPERIMENTS FOR STUDIES OF PROTEIN CONFORMATIONS

Kurt Wüthrich

Institut für Molekularbiologie und Biophysik
Eidgenössische Technische Hochschule
ETH-Hönggerberg, CH-8093 Zürich, Switzerland

CONTENTS:

1. INTRODUCTION

Applications of nuclear magnetic resonance (NMR) in biological research cover a wide spectrum, including studies of structure and conformation of biological macromolecules, investigations of biomembranes, studies of intermediary metabolites in intact, live cells and organs, and imaging of macroscopic objects.[1,2] In all these different areas the use of NMR has gained much momentum from rapid progress in the development of improved instrumentation and methodology. For studies of protein conformations in solution, which is the theme of this presention, the introduction

of ever higher polarizing fields and of Fourier transform techniques was of particular interest. At present, two-dimensional (2D) experiments[3,4] promise to further increase the potentialities of NMR for delineating biomacromolecular structures.[5] In Section 2 this paper starts with a brief survey of fundamental aspects of NMR spectra of proteins. The main part of the paper, Section 3, describes some more recently introduced experiments. Section 4, finally, contains some general comments on the potentialities of modern NMR experiments for studies of protein conformation.

2. NMR SPECTRA OF PROTEINS

2.1. NMR nuclei in polypeptide chains

Polypeptide chains contain three nuclei with spin I = 1/2, which are suitable for high resolution NMR experiments. These are ^{1}H, ^{13}C and ^{15}N. The relative ease of observation of the NMR signals for the different nuclei at constant field is determined by the NMR sensitivities and the isotope abundance.[6] At natural isotope abundance, relative signal intensities are 1 for ^{1}H, $1.7 \cdot 10^{-4}$ for ^{13}C and $3.8 \cdot 10^{-6}$ for ^{15}N. Hence, NMR observation of ^{13}C and ^{15}N is much more difficult than observation of ^{1}H. As a consequence, ^{1}H NMR has played a dominant role in many biological applications. However, with the improved sensitivity of modern Fourier transform (FT) spectrometers, ^{13}C and ^{15}N have recently also become attractive for NMR studies of biopolymers. Besides optimal instrumentation, isotope enrichment can greatly improve the conditions for ^{13}C and ^{15}N NMR experiments, since the natural abundance of these isotopes is only 1.11% and 0.37%, respectively.[6] As an illustration, ^{1}H, ^{13}C and ^{15}N spectra of peptides or proteins are presented in Figs. 1-3.

Fig. 1 shows two natural abundance ^{13}C NMR spectra of the basic pancreatic trypsin inhibitor (BPTI), a small globular protein of molecular weight 6500, which were recorded at two different field strengths. From comparison with the spectra of the individual amino acid residues in model peptides [6-8] the resonances between 0 and 25ppm can be attributed to methyl carbons of the aliphatic amino acid side chains, between 25 and 70ppm to methylene and methine carbons of the side chains and to the backbone α-carbons, between 110 and 160ppm to the aromatic carbons and the guanidinium group of arginine, and between 165 and 185 to the carbonyl and carboxyl carbons of the polypeptide backbone and the side chains. With the use of Fourier transform spectrometers and large sample volumes, observation of proton noise-decoupled ^{13}C NMR spectra of peptides and proteins is readily achieved even at relatively low magnetic fields, and many of the pioneering studies were done at a frequency

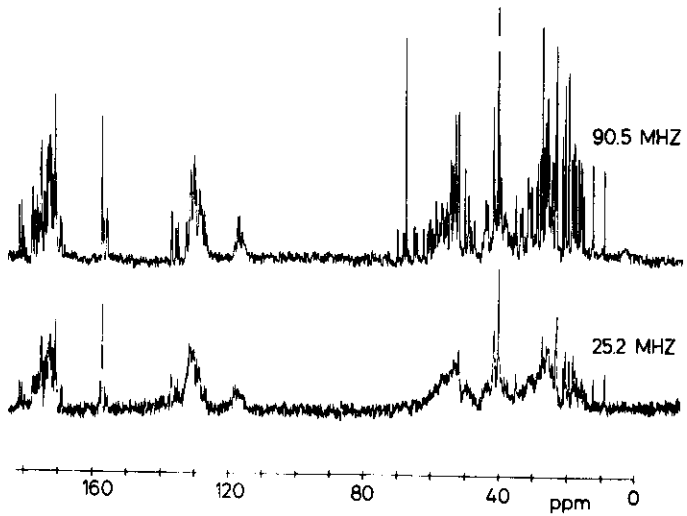

Fig. 1 Natural abundance ^{1}H noise-decoupled FT ^{13}C NMR spectra at 25.2 MHz and 90.5 MHz of a 0.025 M solution of the basic pancreatic trypsin inhibitor (BPTI) in D_2O, pD = 8.2, T = 35° C, accumulation time 12 h. At 25.2 MHz, the sample diameter was 12 mm, 54'000 transients were accumulated with a recycle time of 0.8 s, the digital resolution is 1.25 Hz/point. At 90.5 MHz, the sample size was 10 mm, 86'000 transients were accumulated with a recycle time of 0.5 s, the digital resolution is 2.5 Hz/point. At both frequencies, a digital broadening of 1 s was applied. The chemical shifts are relative to external TMS.[6] (Reproduced from ref. 9).

of 15 MHz.[10,11] Nevertheless, as is illustrated in Fig. 1, greatly improved resolution can be obtained at higher field strength, in particular for the spectral regions which contain resonances of protonated carbon atoms. The use of high fields is of particular interest for assignments of ^{13}C NMR lines by ^{1}H - ^{13}C heteronuclear double resonance techniques, which depend critically also on the resolution of the ^{1}H NMR spectrum.[9,12]

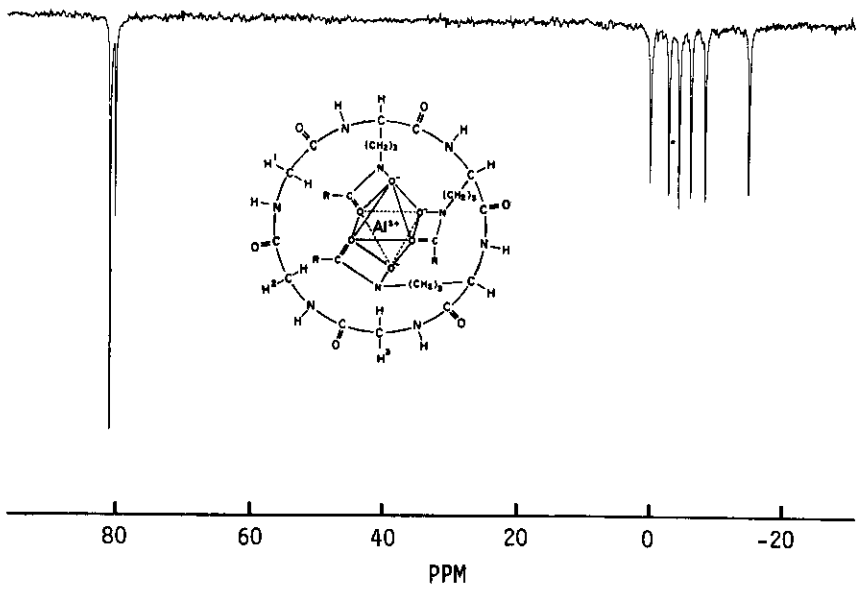

Fig. 2 ^{1}H noise-decoupled FT ^{15}N NMR spectrum at 10.1 MHz of the cyclohexapeptide alumichrome. The spectrum was recorded in ca. 6 h in a 0.07 M solution of 99.2% ^{15}N enriched peptide in deuterated dimethylsulfoxide, T = 45°. The isotope enriched peptide was obtained from a culture of Ustilago sphaerogena which was grown on a medium containing ^{15}N enriched ammonium acetate as the sole nitrogen source. The structure of alumichrome is also indicated in the figure. The backbone peptide nitrogen resonances extend from 0 to approx. -15 ppm and the three metal-coordinated hydroxamate resonances appear at approx. 80 ppm relative to the lowest field amide nitrogen line. The negative sign of the resonance lines is a consequence of the nuclear Overhauser enhancement (NOE). (Reproduced from ref. 13).

Fig. 2 shows the proton noise-decoupled ^{15}N NMR spectrum of a 99% ^{15}N enriched cyclic hexapeptide.[13] When recording proton decoupled ^{15}N spectra, a big gain in sensitivity can be attained through the large negative Overhauser enhancement (NOE).[6,14] Even though natural abundance ^{15}N NMR spectra have been recorded for a variety of peptides and proteins,[15,16] use of ^{15}N labelled molecules appears to be a more promising approach. Particularly attractive experiments can be devised with selective ^{15}N or ^{13}C enrichment of amino acid residues with key roles for the structural and/or functional properties of the protein.[17-19]

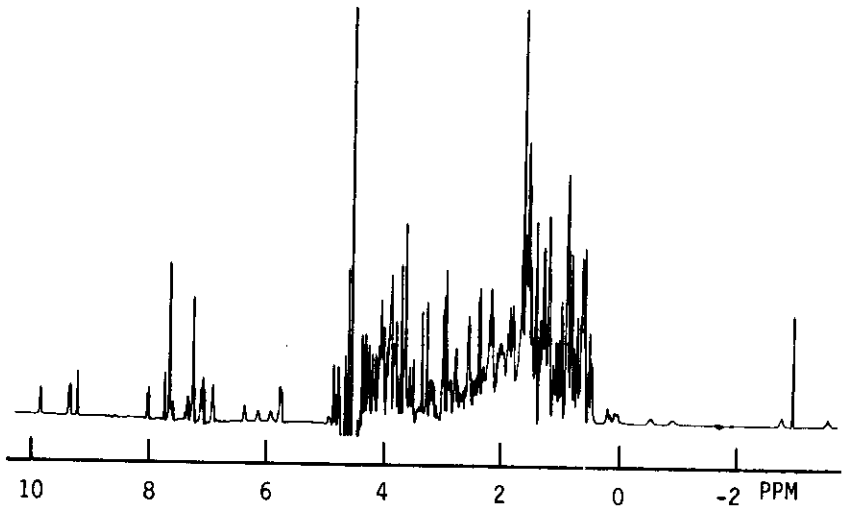

Fig. 3 ^{1}H NMR spectrum at 360 MHz of a 0.002 M solution of ferrocytochrome c-551 from Pseudomonas aeruginosa[21] in 0.05 M deuterated phosphate buffer, pD = 6.6, T = 40°C. This hemoprotein, which has as molecular weight of 8600, consists of one polypeptide chain with 82 amino acid residues and one heme c group. The spectral resolution was improved by multiplication of the free induction decay with a shifted sine bell, $\sin[\pi(t + t_o/t_s)]$, with t_s equal to the acquisition time and $t_o/t_s = 1/64$.

A ^{1}H NMR spectrum of a medium size globular protein is shown in Fig. 3. From comparison with the resonances of the individual amino acid residues,[6,20] peaks between 0 and 2 ppm can be attributed primarily to methyl groups of aliphatic amino acid side chains, between 2 and 3.5 ppm to methine and methylene protons, between 3.5 and 5 ppm to backbone α-protons, and from 6 to 10 ppm to protons of aromatic amino acids and the heme group. The residual solvent protons of HDO give rise to an intense line near 4.5 ppm.[6] The lines between 0 and -4 ppm will be discussed in the following section. Even though high field was used and the resolution was further

improved by digital filtering[6,22,23], the crowded region from 0 to 5 ppm of the spectrum in Fig. 3 is only partially resolved. Compared to ^{13}C and ^{15}N, relatively little can be gained from high resolution ^{1}H NMR studies of proteins at low magnetic fields and therefore advances in the use of ^{1}H NMR were closely linked with the development of high field spectrometers.[6]

2.2. Conformation-dependent ^{1}H NMR chemical shifts

Conformation-dependent chemical shifts arising from interactions of protons with the local magnetic fields of aromatic rings have played an important role in the development of general notions on protein NMR spectra.[6,24] These "ring current shifts" are used here as an illustration for conformation-dependent NMR parameters. Fig.4 shows schematically the ring current field of an aromatic ring. Protons of other segments of the polypeptide chain which are located near the aromatic amino acids in the globular form of the protein, experience the local ring current field, H_R, in addition to the external polarizing field, H_o. The resulting chemical shifts may be as large as ca. 2 ppm for protons near phenylalanine, tyrosine or tryptophan and ca. 5 ppm for protons near porphyrin rings in hemoproteins.[6] Since for a given ring size the extent of the ring current shifts depends only on the relative spatial arrangement of the ring and the observed protons (Fig. 4), conformational features can be clearly manifested in the ring current shifted lines. Thus, in ferrocytochrome c-551 (Fig. 3) the resonances at the high field end of the spectrum are shifted to their extreme positions by the ring current field of the heme group. The five lines between 0 and -4 ppm, where the spectra of diamagnetic organic molecules do not usually contain any resonances,[6] correspond to the methyl and methylene protons of the axially bound methionine side chain (Fig. 5).

On a more general level, "conformation-dependent chemical shifts" are the chemical shift differences for corresponding protons in the globular protein and the random coil form of the polypeptide chain. In a hypothetical "random coil" NMR spectrum of a polypeptide chain computed as the sum of the resonance lines of the constituent amino acid residues measured in small model peptides,[6,20] all the resonance lines are in the spectral regions from ca. 0.8 to 4.8 ppm and 6.8 to 8.2 ppm. They coincide usually closely with the corresponding lines in the experimental spectrum of the denatured protein.[6] In a globular protein, most protons are exposed to local magnetic fields of neighbouring groups in the protein, e.g. aromatic rings (Fig. 4), carbonyl double bonds, etc. Even though most of the local magnetic fields are small compared to the ring current

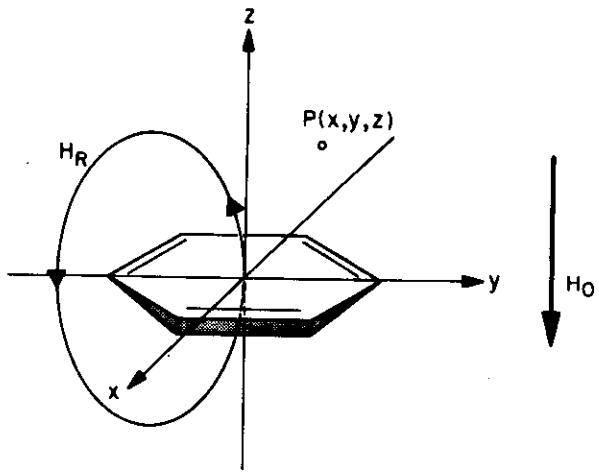

Fig. 4 The local magnetic field of an aromatic ring. H_o is the external polarizing field. For a fixed ring size, the field strength experienced by nearby protons is determined by the position P(x,y,z) relative to the center of the aromatic ring. In a protein, the ring current shifts of nuclei located near aromatic rings are hence determined by the molecular conformation in the environment of the aromatic residue.

fields, they nevertheless cause a dispersion of the chemical shifts about the corresponding random coil values. Since there is generally no periodicity in protein tertiary structures, the local environment of each proton is in general unique, which is manifested by a unique chemical shift in the NMR spectrum. On the one hand this provides that each proton can in principle be observed individually, and hence truly a many-parameter characterization of the protein conformation can be obtained. On the other hand exceedingly complex ^{1}H NMR spectra are obtained even for small and medium size globular proteins, and sophisticated techniques are required to resolve and assign individual resonance lines.

2.3. NMR parameters and protein conformation

In addition to the fore-mentioned manifestations of the spatial polypeptide structure in the chemical shifts, data on protein conformations may be obtained e.g. from spin-spin coupling constants,[25] measurements of spin relaxation parameters, observation of labile

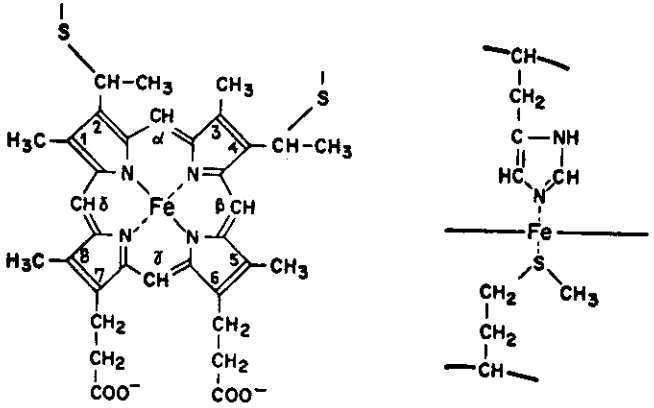

Fig. 5 Heme group (left) and axial ligands of the heme iron (right) in cytochrome c-551. The protons of the axial ligands are located in the area where the ring current field of the porphyrin ring opposes the external field H_o (Fig. 4). As a consequence, in the ^1H NMR spectrum of Fig. 3 the methyl groups and four lines of the four methylene protons of the axial methionine are between 0 and -4 ppm.

protons in D_2O and H_2O solution, and studies of the effects of pH, temperature or shift reagents on the protein NMR spectra.[6] Overall, a wealth of interesting data on differences between protein conformations in different solvent media or between protein crystals and solution,[1,2] on various aspects of protein function[1,2] and, perhaps most important, on internal flexibility of globular proteins[1,2,6,26,27] was thus obtained.

One tackles a considerably more difficult problem when trying to determine the conformation of a polypeptide chain from the known amino acid sequence and the NMR data. The arrangement of a polypeptide chain in space can be characterized e.g. by a complete set of atomic coordinates,[28] by a complete set of torsion angles about all the bonds in the molecular structure[6,28] or by a complete set of intramolecular proton-proton distances.[52] Except in few particularly favorable circumstances, such as the ring current effects near aromatic rings (Fig. 4) or pseudocontact shifts near paramagnetic centers[6,29], the present understanding of NMR chemical

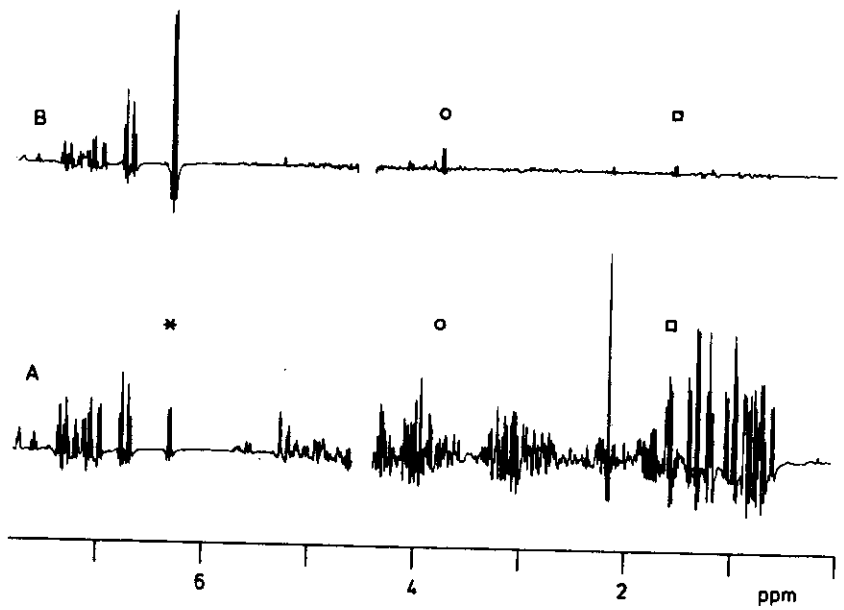

Fig. 6 Selective NOE's between protons of Tyr-23 and Ala-25 (Fig.7) in truncated driven NOE (TOE) difference spectra[34] of BPTI. The figure shows ^1H NMR spectra at 360 MHz of BPTI in D_2O, pD = 7.0, T = 35°C. The spectral resolution was improved by multiplication of the free induction decays with a sine bell.[23] (A) Normal ^1H NMR spectrum. (B) TOE difference spectrum obtained with presaturation of the doublet resonance of the ε-protons of Tyr-23 at 6.30 ppm (*). The multiplets ○ and □ come from Ala-25. (Reproduced from ref. 36).

shifts is not quite sufficient for this parameter to be used systematically for measurements of non-bonding interatomic distances. More direct distance information can be obtained from studies of the manifestations of dipolar spin-spin interactions in the spin relaxation times and in nuclear Overhauser effects (NOE),[6] as will be discussed in more detail in the following section.

3. NEW NMR EXPERIMENTS FOR BIOPOLYMERS IN SOLUTION

3.1. Selective ^1H-^1H Overhauser effects

As was indicated at the end of the foregoing section, studies of nuclear Overhauser enhancements (NOE) appear at present to be

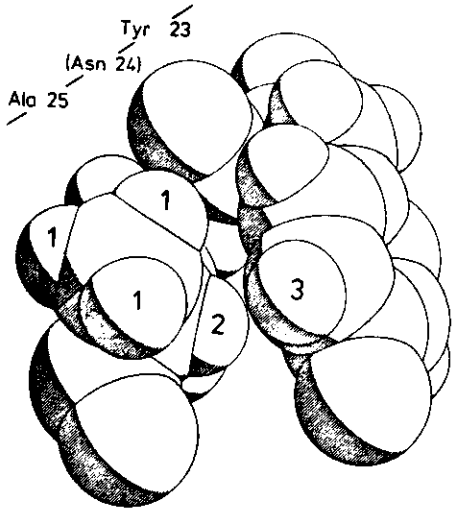

Fig. 7 Computer drawing of the peptide fragment from Tyr-23 to Ala-25 in the refined crystal structure of BPTI.[37] The side chain of Asn-24 was omitted. The size of the individual atoms corresponds to the van der Waals radii. The following atoms are identified by numbers: (1) methyl protons of Ala-25; (2) α-proton of Ala-25; (3) ε-proton of Tyr-23. (Reproduced from ref. 36).

a particularly promising approach for ^1H-^1H distance measurements in proteins, which might eventually provide a sufficient number of intramolecular distance constraints to characterize spatial polypeptide structures. The NOE is the fractional change in intensity by cross relaxation of one NMR line when another resonance is perturbed. It has long been a valuable tool for measurements of internuclear distances in small molecules.[30] In macromolecules at high magnetic fields, however, spin diffusion can become quite efficient[31-33], causing the conventional steady-state NOE's[30] to be less specific and hence less useful. Theory shows that, in contrast, the initial build-up rates of NOE's are simply related to the inverse sixth power of the distance between the observed and the presaturated proton[30-35] and that adverse effects of spin diffusion can be eliminated by suitable selection of the experimental conditions.[33,34] This is illustrated in Fig. 6 which shows selective NOE's between two nearby amino acid side chains (Fig. 7)

in the globular structure of the basic pancreatic trypsin inhibitor (BPTI). The two multiplets (○, □) in the TOE difference spectrum[34] in Fig. 6B indicate close proximity between the side chains of Tyr-23 and Ala-25 in the solution conformation of BPTI. For cytochromes c similar TOE experiments resulted in individual assignments of the heme c proton resonances[21,38] and detailed descriptions of the spatial arrangement of the axial ligands of the heme iron (Fig. 5).[39]

3.2. One-dimensional and two-dimensional NMR

Recent experience has shown that some limitations of conventional, one-dimensional NMR experiments can be overcome with the use of two-dimensional (2D) NMR techniques.[3-5] The experiment of Fig. 6 may serve to illustrate two salient points. Firstly, this particular experiment was successful because the preirradiation was on the well separated line at 6.30 ppm (*), which could selectively be saturated. If instead the preirradiation had been somewhere between 1 and 4 ppm, several resonance lines would have been perturbed simultaneously (Fig. 6), and even without adverse effects of spin diffusion an ambiguous result would have been obtained. Secondly, practical applications of one-dimensional NOE experiments are often discouraged by the low sensitivity, which requires accumulation times of several hours for each individual experiment. Both these difficulties are largely eliminated by 2D NOE spectroscopy (NOESY), which does not require selective preirradiation of individual lines and which yields with a single instrument setting a complete set of selective ^1H-^1H NOE's in a protein.[40] Furthermore, since the resonance peaks are spread out in two dimensions, the spectral resolution at a given field strength H_0 is considerably improved in 2D NMR spectra,[3-5] and it is an important advantage for biological studies that many 2D NMR experiments can be performed nearly as easily in H_2O as in deuterated solvents.[41]

The general principles of 2D spectroscopy[3] provide room for a large number of different 2D NMR experiments.[42] The experiments which are described in the following have so far been particularly useful for work with proteins.

3.3. Two-dimensional correlated spectroscopy

Correlated spectroscopy (COSY)[3], spin echo correlated spectroscopy (SECSY)[43,44] and foldover-corrected correlated spectroscopy (FOCSY)[44] are three 2D NMR experiments for delineating connectivities between J-coupled nuclei. Compared to conventional, one-dimensional spin decoupling experiments, these techniques have the

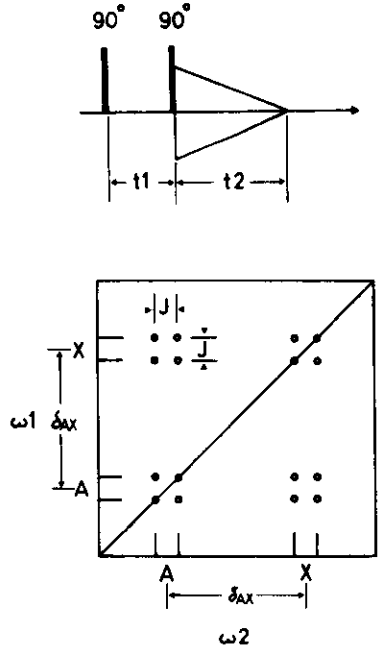

Fig. 8 (A) Experimental scheme for correlated spectroscopy (COSY). The experiment uses two non-selective 90° pulses, which are separated by the "evolution period", t_1. The "detection period", t_2, follows immediately after the second pulse. As in all 2D experiments, the measurement is repeated for a set of equidistant t_1-values.[3] (B) Schematic COSY spectrum for an AX spin system. ω_1 and ω_2 represent the chemical shift on the horizontal and vertical axes. Peaks corresponding to the resonances in the normal, one-dimensional ^{1}H NMR spectrum are on the diagonal. J-connectivities are manifested by cross peaks between the diagonal peaks.

advantage that they do not require selective irradiation of individual multiplets and that a complete set of J-coupling connectivities in a macromolecule can be obtained with a single instrument setting.[3,43,44] The experimental scheme for COSY and a schematic COSY spectrum for an AX spin system are shown in Fig. 8.

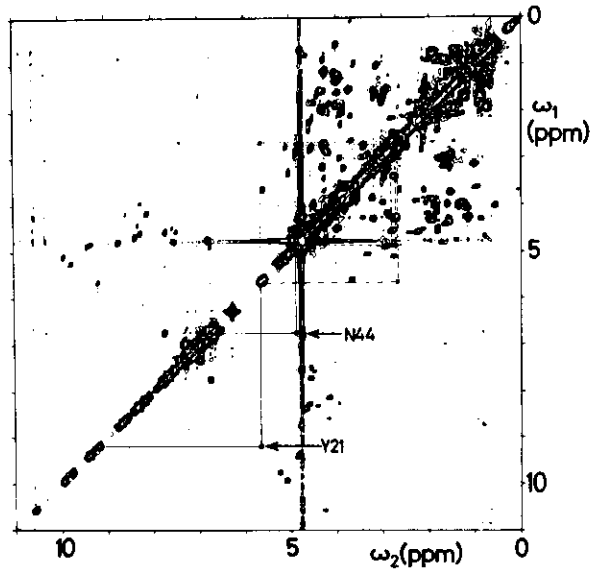

Fig. 9 Contour plot of a 2D correlated (COSY) ^{1}H NMR spectrum at 360 MHz recorded in a 0.02M solution of BPTI in D_2O, pD = 4.6, T = 24°C. An absolute value plot is shown. The residual water protons are observed at 4.8 ppm and cause the appearence of a strong vertical and a weaker horizontal noise band at this position. The peaks on the diagonal correspond to the normal, one-dimensional ^{1}H NMR spectrum.[45] Cross peaks manifesting proton-proton J-connectivities appear in symmetrical locations with respect to the diagonal. The J-connectivities for Tyr-21 and Asn-44 are indicated as follows: ——— Connectivities between amide proton and C^α-proton in the lower triangle. - - - Connectivities between $C^\alpha H$ and $C^\beta H_2$. The two β-protons of Tyr-21 have identical chemical shifts, whereas two separate peaks prevail for $C^\beta H_2$ of Asn-44. ····· Symmetrical connectivities in the upper triangle. (Reproduced from ref. 46).

Fig. 9 shows a COSY spectrum recorded in a solution of BPTI and illustrates how the J-connectivities between protons of the polypeptide backbone and the amino acid side chains can be delineated (for details see figure captions 8 and 9). Note that in addition to the types of protons discussed in Fig. 3, ca. 30 slowly exchanging amide protons with chemical shifts between 6 and 11 ppm are observed in a freshly prepared D_2O-solution of BPTI.[45]

In SECSY and FOCSY spectra the J-connectivity information is presented in different formats.[43,44] SECSY has been used extensively for the identification of the spin systems of amino acid side chains in proteins.[43,44,47]

3.4. Two-dimensional nuclear Overhauser spectroscopy

The experimental scheme for 2D NOE spectroscopy (NOESY)[40,48] is shown in Fig. 10A. It includes three non-selective 90° pulses. After frequency labelling of the various magnetization components during t_1, cross relaxation leads to exchange of magnetization between nearby protons during the mixing time, τ_m. The interval τ_m is kept fixed and the signal recorded immediately after the third pulse as a function of t_2. In the frequency domain spectrum obtained after 2D Fourier transformation of the data set $s(t_1, t_2; \tau_m)$, the diagonal peaks correspond to the resonance positions in the normal, one-dimensional spectrum and NOE's are manifested by pairs of cross peaks in symmetrical locations with respect to the diagonal (Figs. 10B). Since the build-up rates of the NOE's are related to the inverse sixth power of the proton-proton distances[30,33-35], different data sets are generally obtained with different mixing times τ_m.[40] With short mixing times of up to ca. 100msec, only the shortest proton-proton distances likely to occur in a protein will be seen. In NOESY spectra recorded with longer mixing times, say 300msec, additional correlation peaks manifesting longer distances, possibly also via spin diffusion, are likely to occur.[40]

In the NOESY spectrum of BPTI in Fig. 11 a large number of cross peaks can be seen which indicate selective NOE's. The extent of the structural information contained in such a spectrum is indicated by the few cross peaks which are identified in the figure. Firstly, there are NOE's between covalently linked protons of the same amino acid residue, exemplified by the NOE connectivities between $C^{\alpha}H$, $C^{\beta}H$ and $C^{\gamma}H_3$ of Thr-32. Secondly, there are NOE's between the backbone protons of neighbouring residues in the amino acid sequence, illustrated by the cross peaks between $C^{\alpha}H$ and amide protons of residues 30 and 31, and 32 and 33, respectively. Finally there are

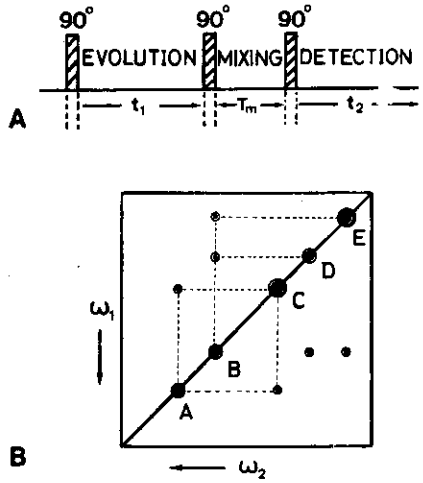

Fig. 10 (A) Experimental scheme for 2D NOE spectroscopy (NOESY).[40,48] The three 90° pulses are separated by the evolution period, t_1, and the mixing period, τ_m. (B) Contour plot of a schematic NOESY spectrum. ω_1 and ω_2 represent the chemical shift (ppm) on the horizontal and vertical axes. Diagonal peaks correspond to the resonance positions in the normal, one-dimensional spectrum. Pairs of symmetrical cross peaks with respect to the diagonal indicate selective NOE's between individual resonance lines, i.e. there are NOE's between A and C, B and D, and B and E. (Reproduced from ref. 40).

the connectivities between protons which are well separated in the covalent structure but closely spaced in the three-dimensional structure. These are illustrated by the cross peaks between the aromatic protons of Tyr-23 and Ala-25, which correspond to the multiplets seen in the TOE difference spectrum of Fig. 6B.

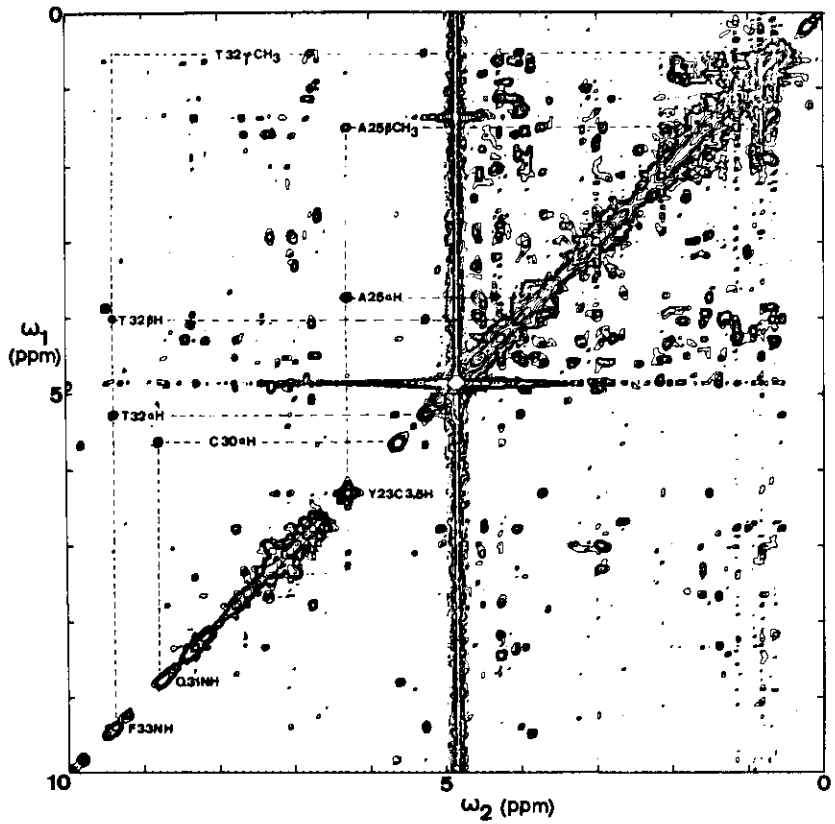

Fig. 11 Contour plot of a 360 MHz ^{1}H NOESY spectrum of BPTI. The protein concentration was 0.02 M, solvent D_2O, pD = 3.8, T = 18°C, the interior amide protons[45] had not been exchanged with deuterium. The mixing time τ_m was 100msec. The absolute value spectrum is shown. NOE connectivities between selected amino acid residues are indicated by the broken lines (see text). These peaks are identified by the one-letter symbol for amino acids (A = alanine, T = threonine, C = cysteine, Q = glutamine, F = phenylalanine, Y = tyrosine), the position in the amino acid sequence and the type of protons observed. The strong vertical spike and the somewhat less intense horizontal spike at 4.8 ppm are due to the resonance of the residual solvent protons. (Reproduced from ref. 40).

3.5. Two-dimensional J-resolved spectroscopy

In a 2D J-resolved spectrum the J-couplings are manifested on a separate frequency axis perpendicular to the chemical shift axis.[5,49] As a consequence, overlap between the individual multiplets is minimized and a considerable improvement of the spectral resolution can be obtained. From 2DJ spectra accurate measurements of spin-spin coupling constants can be obtained even in the most crowded regions of protein ^{1}H NMR spectra.[5,49,50] With the use of 2D J-resolved spectroscopy vicinal spin-spin coupling constants, which have so far mainly been exploited for conformational studies of small peptides,[6,25] thus become accessible also for studies of proteins.[50]

4. CONCLUDING REMARKS ON THE POTENTIALITIES OF NMR TO DETERMINE PROTEIN CONFORMATIONS

Section 2.3. presented briefly some notions on various possible avenues for deriving conformational information from NMR parameters. As indicated there, the NOE experiments described in sections 3.1. and 3.4. provide a particularly straight-forward and generally applicable method, since they allow, without perturbation by extrinsic spectroscopic probes, direct measurements of intramolecular, through-space proton-proton distances.[30-35] Obviously, to represent valid contributions for the determination of the protein conformation, the proton-proton distances must be assigned to specific locations in the amino acid sequence or on prosthetic groups, such as heme c (Fig. 5) in cytochromes c. For an illustration we return to the experiment of Fig. 6. The resonance at 6.3 ppm was assigned to Tyr-23 by chemical modification studies[51] an the A_3X spin system of Ala-25 was identified by sequential resonance assignments using two-dimensional NMR[46]. Since the resonance assignments were thus obtained without reference to the crystal structure, the data of Fig. 6 provide a stringent test that the local conformation in crystalline BPTI shown in Fig. 7 is preserved in solution. If on the other hand the resonances had not been assigned to unique locations in the polypeptide chain, a comparison between crystal and solution would have been highly ambiguous, since BPTI contains 4 tyrosines and 6 alanines.

Generally, when approximate distances between numerous amino acid residues in specified sequence positions can be determined from NOE measurements, quite stringent bounds may result for the conformation space available to the polypeptide chain,[52] whereas in the absence of individual resonance assignments detailed structural interpretation of the NOE data would hardly be warranted.

It is further of crucial importance that, unlike most of the work on protein NMR studies published so far,[1,2,6,29] individual resonance assignments are obtained without reference to single crystal X-ray data. Conceptually it has long been quite obvious that sequential, individual assignments of the NMR lines would be a key to the determination of protein conformations by NMR. Very recently, sequential assignments were to a limited extent obtained by studies of BPTI with one-dimensional ^{1}H NMR techniques,[53] and for the peptide apamin with the use of heteronuclear spin decoupling.[54] However, from the presently available experience[46,47] it is quite clear that the use of the 2D NMR experiments described in sections 3.3. - 3.5. provides a much more powerful and efficient way for obtaining individual resonance assignments for polypeptide chains with known amino acid sequence.

Overall we can conclude that high resolution NMR techniques are presently at a stage where sizeable portions of the three-dimensional structures of small and medium size proteins in solution can be elucidated. This opens the possibility to determine protein conformations when no suitable crystals for X-ray analysis are available. When both crystallography and NMR can be applied, meaningful comparisons of the molecular structures in single crystals and in solution may be obtained. In view of further insights into structure-function correlations, studies of surface residues in globular proteins promise to be particularly fruitful, since surface residues appear to have a tendency to undergo changes in both static and dynamic aspects of conformation between crystal and solution[50,55,56] and are often among the groups involved in the specific functions of globular proteins.[28] X-ray crystallography and NMR can further provide complementary information on dynamic aspects of protein conformations.[26,57-59] NMR studies of internal mobility of proteins have recently been extensively discussed.[6,26,27,50,60-63] With the combined use of the fundamental correlations between NMR parameters and internal molecular flexibility[6] and the many-parameter 2D NMR data sets on protein conformations it should eventually be possible to delineate and localize concerted internal fluctuations, which might be unique for proteins and correlated with specific functional properties.

ACKNOWLEDGEMENTS

Development of 2D NMR techniques for biological studies is a joint project with Prof. R.R. Ernst of the ETH Zürich, which is financed by a special grant of the ETH. This report covers results obtained in collaboration with Drs. Anil Kumar, M. Llinás, K. Nagayama and R. Richarz. Financial support was also obtained from the Swiss National Science Foundation (project 3.528.79). I would like to thank Mrs. E. Huber for the careful preparation of the manuscript.

5. REFERENCES

1. R.A. Dwek, I.D. Campell, R.E. Richards and R.J.P. Williams, eds., NMR in Biology, Academic Press, New York (1977).
2. S.J. Opella and P. Lu, eds., NMR and Biochemistry, Dekker, New York (1979).
3. W.P. Aue, E. Bartholdi and R.R. Ernst, J. Chem. Phys. 64, 2229-2246 (1976).
4. R. Freeman and G.A. Morris, Bull. Magn. Reson. 1, 5-26 (1979).
5. K. Wüthrich, K. Nagayama and R.R. Ernst, Trends in Biochem. Sciences 4, N178-N181 (1979).
6. K. Wüthrich, NMR in Biological Research: Peptides and Proteins, North-Holland, Amsterdam (1976).
7. P. Keim, R.A. Vigna, A.M. Nigen, J.S. Morrow and F.R.N. Gurd, J. Biol. Chem. 248, 7811-7818 (1973).
8. R. Richarz and K. Wüthrich, Biopolymers 17, 2133-2141 (1978).
9. R. Richarz and K. Wüthrich, FEBS Lett. 79, 64-68 (1977).
10. A. Allerhand, R.F. Childers and E. Oldfield, Biochemistry 12, 1335-1341 (1973).
11. A. Allerhand, R.S. Norton and R.F. Childers, J. Biol. Chem. 252, 1786-1794 (1977).
12. R. Richarz and K. Wüthrich, Biochemistry 17, 2263-2269 (1978).
13. M. Llinás and K. Wüthrich, Biochim. Biophys. Acata 532, 29-40 (1978).
14. G.E. Hawkes, W.M. Litchman and E.W. Randall, J. Magn. Reson. 19, 255-258 (1975).
15. D. Gust, R.B. Moon and J.D. Roberts, Proc. Nat. Acad. Sci. 72, 4696-4700 (1975).
16. A. Olesker, L. Valente, L. Barata, G. Lukacs, W.E. Hull, K. Tori, K. Tokura, K. Okabe, M. Ebata and H. Otsuka, Chem. Commun. 577-578 (1978).
17. W.W. Bachovchin and J.D. Roberts, J. Amer. Chem. Soc. 100, 8041-8047 (1978).
18. M.W. Baillargeon, M. Laskowski, D.E. Neves, M.A. Porubcan, R.E. Santini and J.L. Markley, Biochemistry 19, 5703-5710 (1980).
19. R. Richarz, H. Tschesche and K. Wüthrich, Biochemistry 19, 5711-5715 (1980).
20. A. Bundi and K. Wüthrich, Biopolymers 18, 285-297 (1979).
21. R.M. Keller and K. Wüthrich, Biochem. Biophys. Res. Commun. 83, 1132-1139 (1978).
22. R.R. Ernst, Advan. Magn. Reson. 2, 1-135 (1966).

23. A. De Marco and K. Wüthrich, J. Magn. Reson. 24, 201-204 (1976).
24. C.C. McDonald and W.D. Phillips, J. Amer. Chem. Soc. 89, 6332-6341 (1967).
25. V.F. Bystrov, Progress in NMR Spectroscopy 10, 41-81 (1976).
26. K. Wüthrich and G. Wagner, Trends Biochem. Sciences 3, 227-230 (1978).
27. G. Wagner and K. Wüthrich, J. Mol. Biol. 134, 75-94 (1979).
28. G.E. Schulz and R.H. Schirmer, Principles of Protein Structure, Springer-Verlag, New York (1979).
29. R.A. Dwek, Nuclear Magnetic Resonance (NMR) in Biochemistry, Clarendon Press, Oxford (1973).
30. J.H. Noggle and R.E. Schirmer, The Nuclear Overhauser Effect, Academic Press, New York (1971).
31. A. Kalk and H.J.C. Berendsen, J. Magn. Reson. 24, 343-366 (1976).
32. W.E. Hull and B.D. Sykes, J. Chem. Phys. 63, 867-880 (1975).
33. S.L. Gordon and K. Wüthrich, J. Amer. Chem. Soc. 100, 7094-7096 (1978).
34. G. Wagner and K. Wüthrich, J. Magn. Reson. 33, 675-680 (1979).
35. A.A. Bothner-By and J.H. Noggle, J. Amer. Chem. Soc. 101, 5152-5155 (1979).
36. K. Wüthrich, G. Wagner, R. Richarz and S.J. Perkins, Biochemistry 17, 2253-2263 (1978).
37. J. Deisenhofer and W. Steigemann, Acta Crystallogr. B 31, 238-250 (1975).
38. R.M. Keller and K. Wüthrich, Biochim. Biophys. Acta 533, 195-208 (1978).
39. H. Senn, R.M. Keller and K. Wüthrich, Biochem. Biophys. Res. Commun. 92, 1362-1369 (1980).
40. Anil Kumar, R.R. Ernst and K. Wüthrich, Biochem. Biophys. Res. Commun. 95, 1-6 (1980).
41. Anil Kumar, G. Wagner, R.R. Ernst and K. Wüthrich, Biochem. Biophys. Res. Commun. 96, 1156-1163 (1980).
42. R.R. Ernst, W.P. Aue, P. Bachmann, A. Höhner, M. Linder, B. Meier, L. Müller, A. Wokaun, K. Nagayama and K. Wüthrich, Proceedings of the XXth Congress Ampère, Tallinn, 15-18 (1978).
43. K. Nagayama, K. Wüthrich and R.R. Ernst, Biochem. Biophys. Res. Commun. 90, 305-311 (1979).
44. K. Nagayama, Anil Kumar, K. Wüthrich and R.R. Ernst, J. Magn. Reson. 40, 321-334 (1980).
45. K. Wüthrich and G. Wagner, J. Mol. Biol. 130, 1-18 (1979).
46. G. Wagner, Anil Kumar and K. Wüthrich, Eur. J. Biochem. 114, 375-384 (1981).
47. K. Nagayama and K. Wüthrich, Eur. J. Biochem. 114, 365-374 (1981).
48. J. Jeener, B.H. Meier, P. Bachmann and R.R. Ernst, J. Chem. Phys. 71, 4546-4553 (1979).

49. K. Nagayama, P. Bachmann, K. Wüthrich and R.R. Ernst, J. Magn. Reson. 31, 133-148 (1978).
50. K. Nagayama and K. Wüthrich, Eur. J. Biochem. (1981) in the press.
51. G.H. Snyder, R. Rowan III, S. Karplus and B.D. Sykes, Biochemistry 14, 3765-3777 (1976).
52. W. Braun, Ch. Bösch, L.R. Brown, N. Gō and K. Wüthrich, Biochim. Biophys. Acta 667, 377-396 (1981).
53. A. Dubs, G. Wagner and K. Wüthrich, Biochim. Biophys. Acta 577, 177-194 (1979).
54. V.V. Okhanov, V.A. Afanas'ev and V.F. Bystrov, J. Magn. Reson. 40, 191-195 (1980).
55. L.R. Brown, A. De Marco, G. Wagner and K. Wüthrich, Eur. J. Biochem. 62, 103-107 (1976).
56. L.R. Brown, A. De Marco, R. Richarz, G. Wagner and K. Wüthrich, Eur. J. Biochem. 88, 87-96 (1978).
57. P.J. Artymiuk, C.C.F. Blake, D.E.P. Grace, S.J. Oatley, C.D. Phillips and M.J.E. Sternberg, Nature 280, 563-568 (1979).
58. H. Frauenfelder, G.A. Petsko and D. Tsernoglou, Nature 280, 558-563 (1979).
59. R. Huber, Trends Biochem. Sciences 4, 271-276 (1979).
60. A. Allerhand, Methods in Enzymology 61, Enzyme Structure, Part H, 458-508 (1979).
61. O. Jardetzky, Biochim. Biophys. Acta 621, 227-232 (1980).
62. R. Richarz, K. Nagayama and K. Wüthrich, Biochemistry 19, 5189-5196 (1980).
63. A.A. Ribeiro, R. King, C. Restivo and O. Jardetzky, J. Amer. Chem. Soc. 102, 4040-4051 (1980).